© APR 2026 | IRE Journals | Volume 9 Issue 10 | ISSN: 2456-8880
DOI: https://doi.org/10.64388/IREV9I10-1716943

Sustainable Synthesis of Calcium Carbonate (CaCO3) from Periwinkle Shells for Efficient Methylene Blue Removal

T. E. AMAKOROMO[1], P. S. COOKEY[2]
[1]*Department of Physics Electronics Technology, University of Port Harcourt, Rivers State, Nigeria.*
[2]*Department of Physics Electronics Technology, Federal Polytechnic of Oil and Gas, Bonny, Rivers State, Nigeria*

Abstract- ***The ability of CaCO3 to sequester methylene blue (MB) from water was assessed through spectrophotometric, kinetic, and isotherm studies. The adsorption process was greatly affected by pH, with the best results at pH 7.5. This is due to deprotonation of surface functional groups and stronger electrostatic attraction to positively charged dye molecules. An optimal amount of adsorbent at 1.500 g/L achieved about 83% removal, showing more active sites become available until saturation. Isotherm results indicated a strong affinity between MB and the adsorbent, with removal rates over 90% at low initial concentrations. At higher concentrations (40–100 mg/L), removal efficiency dropped as active sites became saturated. Nevertheless, the adsorbent still removed over 80% of the dye across the tested range, proving its durability and effectiveness. These findings suggest that modified CaCO3 is a promising, eco-friendly adsorbent for dye-laden wastewater treatment and offers a valuable use for periwinkle shells, which are usually waste.***

Key words: Sequestration, Methylene blue, Dye Removal, CaCO3, Periwinkle Shell

I. INTRODUCTION

Complex wastewater discharge into natural aquatic environments has significantly increased due to rapid global industrialisation. A serious environmental catastrophe, marked by the release of complex, hazardous effluents into aquatic ecosystems, has been unintentionally caused by industries such as textiles, printing, paper, and leather. (Husien et al., 2022). Due to the high stability and resilience of heavy metals and synthetic dyes to natural degradation, they pose a complex hazard to human health and ecological integrity when they contaminate water. (Alprol et al., 2025). Synthetic dyes used to color textiles, leather, and plastics are among the many contaminants found in industrial wastewater that are especially dangerous because of their high visibility even at low concentrations and their potential to cause cancer and mutagenesis (Alvez-Tovar et al., 2025). A primary culprit within this industrial waste stream is Methylene Blue (MB), a common cationic heterocyclic aromatic chemical used as a coloring agent in the textile industry. MB is classified as a detrimental pollutant despite its extensive industrial use due to its environmental persistence and acute toxicity to humans and aquatic life. Numerous physiological conditions, such as respiratory discomfort, gastrointestinal irritation, mental disorientation, and methemoglobinemia, might result from exposure to MB-contaminated water (Ho, 2020; Muteeb et al., 2025). According to Al-Asadi et al. (2025) and Alvez-Tovar et al. (2025), the presence of such dyes in water bodies also hinders light penetration, which disrupts photosynthetic activities of aquatic flora and lowers dissolved oxygen levels, ultimately destabilizing the aquatic food chain. In response to the severity of this dye pollution, the scientific community has made developing effective and sustainable wastewater treatment technologies a top priority. The effectiveness of conventional remediation techniques in eliminating organic dyes has been assessed (Ho, 2020). Early filtration methods relied on rudimentary physical barriers, but in the middle of the 20th century, chemical precipitation and sophisticated oxidation became common filtration techniques, replacing the crude physical barriers used in earlier approaches. However, these processes frequently result in the production of secondary hazardous sludge and substantial operating costs (Nhung et al., 2023). On the other hand, adsorption has become a leading method for wastewater purification due to its straightforward design, great efficiency, affordability, and potential for adsorbent regeneration (Pathania et al., 2013). The

development of adsorbents has progressed through several stages, each characterized by the complexity and source of the materials used. These technological generations have influenced our current knowledge and understanding of pollutant capture. Commercial activated carbons, which are efficient but have high production costs and carbon-intensive activation methods, were the main source of first-generation adsorbents (Tabassum et al., 2024). The focus of second-generation materials changed to naturally occurring minerals such zeolites and clays, which offered a less selective but more affordable option (Abd Elnabi et al., 2023; Nhung et al., 2023). Engineered nanomaterials, such as carbon nanotubes and metal-organic frameworks (MOFs), were introduced by third-generation developments. Despite their remarkable surface areas, complex synthesis pathways and the precursors' possible environmental toxicity sometimes impede their practical utilization (Senthil Rathi et al., 2024). Fourth-generation adsorbents, the current frontier, concentrate on biogenic minerals obtained from marine and agricultural waste. This method, which turns discarded biological materials into valuable environmental instruments, is consistent with the "waste-to-wealth" mindset. Among them, biogenic calcium carbonate ($CaCO_3$) has become a ground-breaking contender, providing a special blend of abundant surface functionalization, biocompatibility, and structural integrity (Maruyama, 2024). A sustainable source of $CaCO_3$ that avoids the environmental costs of geological mining is provided by the valorization of seafood waste, particularly the shells of gastropods. In the Niger Delta's coastal regions, the periwinkle (*Tympanotonus fuscatus*) is a major food staple, which leads to the accumulation of enormous amounts of shell waste. These shells are frequently thrown away carelessly, adding to environmental litter and clogging drainage systems (Elegbede et al., 2023; Nkwoada, et al., 2021). From a chemical standpoint, these shells, which are usually found in the aragonite or calcite polymorphs, are a veritable gold mine of biogenic $CaCO_3$. The biological origin of this mineral gives it a rich density of surface active sites and a natural porosity that are frequently better than those of their synthetic counterparts (Nwaeju et al., 2025; Tabassum et al., 2024). Through a number of physicochemical interactions, these characteristics enable the quick capture and stabilization of Methylene Blue (Kargule, et al., 2025). A periwinkle-derived adsorbent's performance is mostly dependent on its structural design. According to Kedir et al. (2023), the biogenic $CaCO_3$ matrix offers a strong scaffold with a variable pore size distribution and a heterogeneous surface. The carbonate and hydroxyl groups that adorn these mineral surfaces serve as binding sites for the cationic dye molecules. In addition to hydrogen bonding and π-π stacking interactions, the interaction is mainly driven by electrostatic attraction between the positively charged MB cations and the negatively charged adsorbent surface (Maruyama, 2024). Additionally, these shells can be thermally modified to convert the $CaCO_3$ into calcium oxide (CaO), which has even greater reactivity and adsorption capacity under certain aqueous circumstances (Kedir et al., 2023). These materials are usually synthesized using three main methods: mechanical activation, thermal calcination, and chemical modification. For periwinkle shells, thermal treatment works especially well since it eliminates the organic conchiolin matrix and improves the crystallinity of the mineral phase (Nwaeju et al., 2025). Advanced fabrication techniques, including ultrasonic assisted synthesis and hydrothermal processing, have been explored in the period between 2020 and 2026 to further refine the particle size and surface area of the biogenic carbonate (Senthil Rathi et al., 2024). These improvements are critical for transitioning from laboratory-scale experiments to industrial-scale water purification modules.

This research focuses on the synthesis and optimization of biogenic calcium carbonate from *Tympanotonus fuscatus* shells for the targeted removal of Methylene Blue. The work concurrently tackles two environmental issues: the management of solid marine garbage and the cleanup of dye-contaminated water, by utilizing the inherent structural benefits of these shells. In order to provide a scalable model for sustainable wastewater treatment, a comprehensive kinetic, isothermal, and thermodynamic investigations will be used to evaluate the efficacy of the resultant adsorbent, offering insights into the adsorption mechanism and the possibility of widespread use in industrial wastewater treatment. This study adds to the global effort to incorporate biogenic waste into the circular economy for environmental protection

© APR 2026 | IRE Journals | Volume 9 Issue 10 | ISSN: 2456-8880
DOI: https://doi.org/10.64388/IREV9I10-1716943

through thorough characterization and performance evaluation.

II. MATERIALS AND METHODS

2.1 Synthesis of $CaCO_3$ from Periwinkle Shells

Periwinkle shells, a common seafood waste primarily composed of calcium carbonate (CaCO3), were obtained from vendors at Choba Market. The shells were washed repeatedly with tap water, then with distilled water, to remove debris and visible organic matter. Samples were air-dried for 72 hours (Fig 1) and then oven-dried for 24 hours at 60 °C (Fig 2). The dried shells were crushed and ground into a powder using a commercial blender, then sieved through analytical-grade sieves of 150, 300, and 600 microns. The 150-micron fraction, representing the finest particles, was selected for further processing. These samples were subjected to thermal treatment in a muffle furnace at 600 °C, followed by treatment with H2SO4 to produce modified CaCO3.

To study the material's progression, FTIR and XRD analyses were conducted.

Fig. 1: Air-dried periwinkle shells

Fig. 2: Oven-Drying of samples

2.2 Adsorbent Preparation

The following sections outline the preparation steps and experimental procedures employed in this study, presenting a systematic progression from sample preparation to analysis.

2.2.1 MB Stock Solution Preparation

A 1000 mg/L stock solution of Methylene Blue (MB) was prepared by dissolving an accurately weighed amount of MB powder (Merck (Sigma-Aldrich), Analytical grade (AR), ≥82% purity, molecular weight 319.86 g/mol) in distilled water. This stock solution was subsequently diluted to obtain a 50 mg/L MB solution for kinetic and dose experiments. For isotherm studies, MB solutions at concentrations of 25, 50, 100, 150, 200, and 300 mg/L were prepared by serial dilution. All solutions were adjusted to pH 7 using 0.1 M NaOH or 0.1 M HCl. All chemicals were analytical grade and used without further purification.

2.2.2 Calibration Curve Development

The UV-Vis spectrophotometer (Searchtech Instruments, England, Type 721) was set to 664 nm to measure the maximum absorbance of MB. Baseline correction was performed using a quartz cuvette containing distilled water. Calibration curves were constructed using standard MB solutions at concentrations of 0, 2, 5, 10, 15, 20, 30, and 50 mg/L. Absorbance values were measured in triplicate, and the mean values were plotted as Absorbance versus Concentration. Linear regression was used to derive the calibration equation.

$$Y = mX + c \qquad (1)$$

where Y stands for absorbance, X for concentration (mg/L), m for slope, and c for intercept.

2.3 Adsorption Experiments

2.3.1 Experiment A: Adsorption Kinetics and Equilibrium Time

This experiment was designed to determine the time required for the adsorption process to reach equilibrium. Fifty milliliters of a 50 mg/L methylene blue (MB) solution were distributed into 8–10 flasks, each containing 0.1 g/L of adsorbent (5 mg CaCO3). The pH was adjusted to 7, and the mixtures were agitated in an isothermal water bath shaker (Memmert, model WNB7-45, Germany) at 150 rpm and room

© APR 2026 | IRE Journals | Volume 9 Issue 10 | ISSN: 2456-8880
DOI: https://doi.org/10.64388/IREV9I10-1716943

temperature. Time zero was recorded at the start of agitation. At predetermined intervals (5, 15, 30, 60, 120, 240, 480, and 1440 minutes), flasks were removed, filtered through Whatman No. 4 filter paper (20 µm pore size), and the filtrate absorbance was measured at 664 nm. The concentration at each time point (Ct) was determined using the calibration curve. The removal percentage was calculated using the specified equation.sing the specified equation.

$$\%\ Removal = \frac{C_o - C_t}{C_o}\ x\ 100 \qquad (2)$$

The resulting data were analysed by plotting percentage removal against time to identify the point at which the curve plateaued, which indicated the equilibrium time for subsequent experiments.

2.3.2 Experiment B: Optimisation of Adsorbent Dosage

To determine the optimal adsorbent mass for the adsorption process, the CaCO3 dose was varied across five flasks under constant conditions. Each flask contained 50 mL of a 50 mg/L methylene blue (MB) solution mixed with 10, 25, 50, 75, or 100 mg of CaCO3, corresponding to adsorbent doses of 0.2, 0.5, 1.0, 1.5, and 2.0 g/L. After agitation at 150 rpm at room temperature for the established equilibrium time, the mixtures were filtered, and the final concentrations (Ce) were determined by measuring the absorbance of the filtrate. The results were analyzed by plotting percentage removal against adsorbent dose, and the dose immediately preceding the plateau was designated as the optimum.

2.3.3 Experiment C: Adsorption Isotherm Study

Adsorption isotherms were investigated to determine the maximum adsorption capacity of CaCO3 using 6–8 flasks, each containing 50 mL of MB solution at concentrations ranging from 25 to 300 mg/L. The optimum adsorbent dose identified in Experiment B was added to each flask. Samples were agitated for the equilibrium time established in Experiment A at pH 7, then filtered. The equilibrium concentration (Ce) was measured by spectrophotometry. Initial and final MB concentrations were determined using the calibration curve. Percentage removal was calculated using Equation (2), and the amount adsorbed at equilibrium, qe (mg/g), was calculated using the mass balance equation (3).

where C_o is the initial concentration (mg/L), C_e is the equilibrium concentration (mg/L), V is the volume of solution (L), and m is the mass of adsorbent (g).

2.4 Statistical Analysis

All experiments were performed in triplicate, and results are reported as mean ± standard deviation. Non-linear regression was applied for isotherm modeling, and linear regression was used for calibration curves. Correlation coefficients (R2) were calculated to assess the goodness of fit.

III. RESULTS AND DISCUSSION

The FTIR spectra of raw periwinkle shell powder (Fig. 3) demonstrate a clear dominance of inorganic carbonate ($CaCO_3$) peaks at 712, 857, and 2519 cm^{-1}. In contrast, the peaks at 1080, 1446, and 1647 cm^{-1} indicate the presence of organic components derived from the shell's biological matrix.

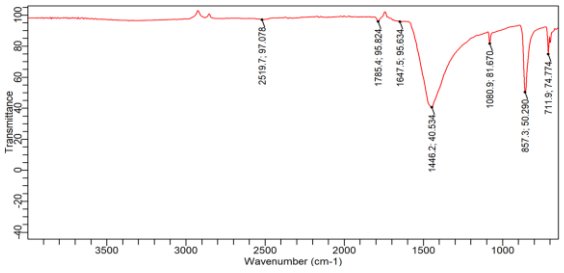

Fig.3: FTIR Spectrum of raw periwinkle shells

The CaCO3 peaks (Fig. 4) persisted following thermal treatment at 600 °C, indicating the thermal stability of the material. In contrast, the peaks at 1080, 1446, 1647, and 1785 cm^{-1}, which correspond to organic functional groups in the raw samples, were eliminated. These findings confirm the effectiveness of the pyrolysis process.

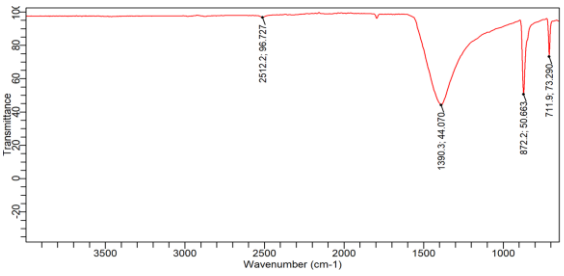

Fig.4: FTIR Spectrum of samples after heat treatment at 600 °C

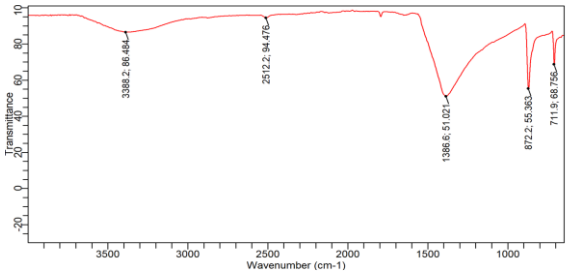

Fig.5: FTIR Spectrum of samples after acid treatment

After acid treatment(with H_2SO_4), the O-H functional group was identified showing strong structural change and modification.

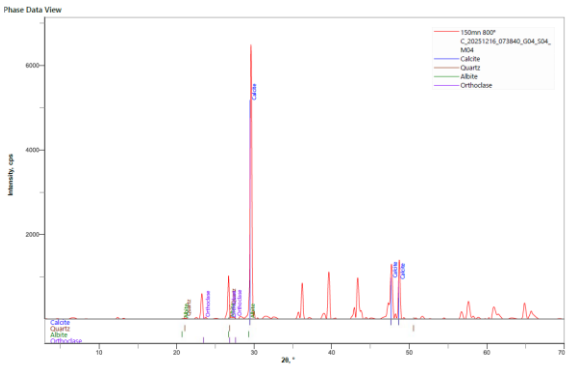

Fig 6.: XRD structure of acid treated samples.

It was observed that while the material remained $CaCO_3$, throughout the treatment stages, the XRD revealed the phase change.

3.2 Optical Calibration and Linear Response Characteristics

The creation of a standard calibration curve provided a linear basis for the quantitative measurement of Methylene Blue (MB) sequestration. Spectrophotometry at a fixed wavelength of 664 nm was used to analyze standard solutions with known MB concentrations. Table 1 displays the recorded absorbance values for concentrations between 2 mg/L and 30 mg/L, which range from 0.473 to 1.981 nm. The accurate conversion of subsequent experimental absorbance data into precise concentration metrics depends on this linear relationship.

Table 1. Absorbance values for MB standard solutions at 664 nm

Conc (mg/l)	Abs (nm)
2	0.473
5	0.871
10	1.452
15	1.880
20	1.944
30	1.981

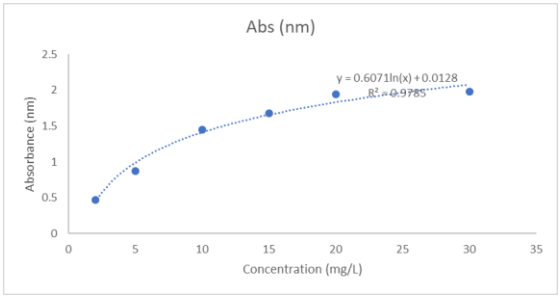

Fig. 7 Calibration Curve (Graph of Absorbance vs. Concentration illustrating the linear response of Methylene Blue at 664 nm and the derivation of the calibration equation)

The findings showed that absorbance increased in direct proportion to dye concentration, indicating a high level of spectrophotometric accuracy. The final concentrations (Ce) and removal percentages in the kinetic and dose trials can be computed using the resulting linear equation, y=0.6198 ln(x)+0.3139, which has a correlation coefficient (R2) of 0.9559.

3.2 Adsorption Kinetics and Removal Efficiency

The system's equilibrium time was determined by analysing the carbon-based adsorbent's kinetic activity. The percentage clearance values in Table 2 show rapid initial uptake in the experimental results at an initial MB concentration of 50 mg/L. Within the first 10 minutes, the removal efficiency was 70.53%, and after 80 minutes it stabilised at almost 79%. This plateau is consistent with saturation of active sites on the adsorbent surface. This pattern is shown in the kinetic plot in Fig 7, which displays a steep initial rise followed by a stable equilibrium phase at 80 minutes.

© APR 2026 | IRE Journals | Volume 9 Issue 10 | ISSN: 2456-8880
DOI: https://doi.org/10.64388/IREV9I10-1716943

Table 2. Kinetic data for MB adsorption (C_0 = 50 mg/L, Dose = 0.1 g/L)

TIME (MINS)	ABS. (NM)	MB CONC. (MG/L)	% REMOVAL
10	1.336	8.842	70.526
20	1.220	7.304	75.652
40	1.182	6.861	77.129
60	1.140	6.403	78.658
80	1.130	6.298	79.007
100	1.132	6.319	78.938
120	1.137	6.371	78.763

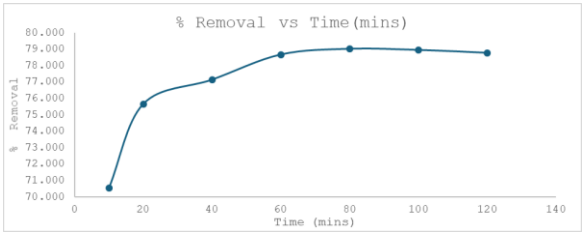

Fig. 8. Relationship between adsorbent dosage and percentage removal of MB

3.3 Effect of Adsorbent Dosage on Removal Performance

To determine the optimum adsorbent dose for maximum sequestration efficiency, the link between adsorbent mass and dye elimination was examined. Table 3 summarizes the absorbance and removal percentages obtained by varying the dosage from 0.200 g/L to 2.000 g/L. It was observed from the dose curve Fig 8 that as the dose was raised from 0.200 g/L to 1.500 g/L, there was a gradual improvement in removal efficiency from 63.43% to 82.52% Nevertheless, a minor drop in removal was noted at 2.000 g/L (80.345%). This indicates that an overdose of adsorbent may cause particle aggregation, hence decreasing the number of active sites that are available and that as the system gets closer to saturation, the marginal increases in elimination efficiency diminish beyond 1.0 g/L. As a result, the optimum dosage for this system was found to be 1.500 g/L.

Table 3 Effect of varying adsorbent dose on MB removal (C0 = 50 mg/L)

Ads Dose (g/L)	Abs (nm)	MB Conc	% Removal
0.200	1.467	10.972	63.428
0.500	1.142	6.424	78.588
1.000	1.019	5.246	82.515
1.500	1.004	5.118	82.941
2.000	1.090	5.896	80.345

3.5 The Optimum Adsorption Capacity

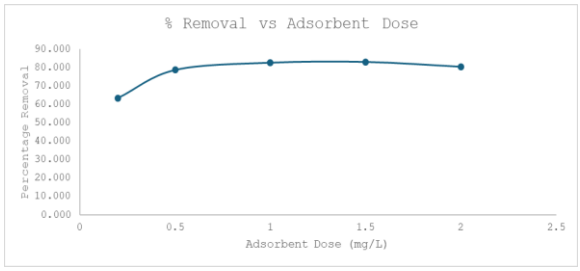

Fig 9. Relationship between adsorbent dosage and percentage removal of MB, highlighting the plateau effect and optimum dosage point

3.4 MB Adsorption Isotherm Performance

The adsorption performance of the synthesized material was evaluated across a wide range of initial Methylene Blue (MB) concentrations (10–100 mg/L) at a constant pH of 7. The batch experiments were conducted using a 50 mL volume per flask and the pre-determined optimum adsorbent dose (1.500 g/L.) and equilibrium contact time (80 minutes). The results for the final equilibrium concentrations (Ce) and the corresponding removal efficiencies are summarized in Table 4

Table 4. Experimental data for MB adsorption isotherm

Initial Conc (mg/L)	Initial abs	Final Abs	Final Conc (mg/L)	% Removal
10	0.756	0.181	1.319	86.808
20	1.083	0.394	1.874	90.632
30	1.553	0.624	2.737	90.878

40	1.628	0.912	4.398	89.005
50	1.644	1.243	7.586	84.827
60	1.706	1.487	11.339	81.101
80	1.818	1.646	14.734	81.582
100	1.932	1.795	18.833	81.167

The results from Table 1 indicate that the removal efficiency of MB increases with higher initial concentrations up to a peak of 90.878% at 30 mg/L. Beyond this concentration, further increases lead to decreased removal efficiency, dropping to 81.167% at 100 mg/L. Additionally, the final equilibrium concentration (C_e) rises consistently from 1.319 mg/L to 18.833 mg/L as the initial concentration increases.

3.5 Discussion

The spectrophotometric and kinetic analyses reveal the sequestration potential of the synthesized adsorbent. The optical calibration ensures accurate removal percentage calculations. Kinetic studies show that pH significantly impacts performance, with enhanced removal at pH 7.5 due to the deprotonation of surface functional groups, increasing the attraction between the adsorbent and cationic MB molecules. The sequestration efficiency is optimized at a dosage of 1.500 g/L, achieving approximately 83% removal of the organic dye. This indicates that increased adsorbent doses create more active sites until reaching a saturation point, after which aggregation may happen. The adsorption isotherm analysis indicates a high interaction between MB molecules and the adsorbent surface, with removal efficiency exceeding 90% at lower concentrations, demonstrating a strong affinity for the dye and sufficient active sites on the material, The decrease in removal percentage at higher initial concentrations (40 mg/L to 100 mg/L) is due to the saturation of active binding sites as the concentration of MB molecules increases. This indicates a reduction in the available surface area relative to the total solute amount. Nonetheless, the material exhibited strong performance, with removal efficiencies exceeding 80% throughout the tested range, confirming its effectiveness as an adsorbent for wastewater treatment applications. This work advances the development of sustainable dye-removal methods by bridging thorough performance characterization with strict experimental control.

REFERENCES

[1] Abd Elnabi, M. K., Elkaliny, N. E., Elyazied, M. M., Azab, S. H., Elkhalifa, S. A., Elmasry, S., Mouhamed, M. S., Alhorieny, N. A., Abd Elaty, A. E., Elgendy, I. M., Etman, A. E., Saad, K. E., Tsigkou, K., Ali, S. S., Kornaros, M., & Mahmoud, Y. A.-G. (2023). Toxicity of heavy metals and recent advances in their removal: A review. Toxics, 11(7), 580. https://doi.org/10.3390/toxics11070580

[2] Al-Asadi, S. T., Mussa, Z. H., Al-Qaim, F. F., Kamyab, H., Al-Saedi, H. F. S., Deyab, I. F., & Kadhim, N. J. (2025). A comprehensive review of methylene blue dye adsorption on activated carbon from edible fruit seeds: A case study on kinetics and adsorption models. *Carbon Trends*, 20, 100507. https://doi.org/10.1016/j.cartre.2025.100507

[3] Alprol, A. E., Manaa, A., Basaham, A. S., Ghandour, I. M., Abu El-Regal, M. A., & El-Metwally, M. E. A. (2025). Optimized removal of methylene blue from wastewater using an activated Carbon-Zinc Oxide-Ammonia composite. *Scientific Reports*, *15*(1), 38834. https://doi.org/10.1038/s41598-025-08783-9

[4] Alvez-Tovar, B., Scalize, P. S., Angiolillo-Rodríguez, G., Albuquerque, A., Ebang, M. N., & de Oliveira, T. F. (2025). Agro-industrial waste upcycling into activated carbons: A sustainable approach for dye removal and wastewater treatment. *Sustainability, 17*(5), 2036. https://doi.org/10.3390/su17052036

[5] Elegbede, I. O., Lawal-Are, A., Oloyede, R., Sanni, R. O., Jolaosho, T. L., Goussanou, A., & Ngo-Massou, V. M. (2023). Proximate, minerals, carotenoid and trypsin inhibitor composition in the exoskeletons of seafood gastropods and their potentials for sustainable circular utilisation. Scientific Reports, 13, 11155. https://doi.org/10.1038/s41598-023-38345-w

[6] Ho, S.-M. (2020). Removal of dyes from wastewater by adsorption onto activated carbon: Mini review. *Journal of Geoscience and*

Environment Protection, *8*(5), 120–131. https://doi.org/10.4236/gep.2020.85008

[7] Husien, S., El-taweel, R. M., Salim, A. I., Fahim, I. S., Said, L. A., & Radwan, A. G. (2022). Review of activated carbon adsorbent material for textile dyes removal: Preparation, and modelling. *Current Research in Green and Sustainable Chemistry,* 5, 100325. https://doi.org/10.1016/j.crgsc.2022.100325

[8] Kargule, B.B., Al-Asadi, M., Al-Anssari, S., Aljibori, H.S.S., Hamzah, H.T., Tastambek, K.T., Abdullah, T.A., & Abdullah, O.I. (2025). Sustainable removal of dyes from wastewater using eggshell-derived calcium carbonate nanoparticles: Adsorption isotherms, Kinetics, and Thermodynamic Analysis Supporting Sustainable Development Goals (SDGs). ASEAN Journal of Science and Engineering, 5(2), 369-394. DOI:10.17509/ajse.v5i2.88499

[9] Kedir, W. M., Wondimu, K. T., & Weldegrum, G. S. (2023). Optimization and characterization of biodiesel from waste cooking oil using modified CaO catalyst derived from snail shell. Heliyon, 9(5), e16475. https://doi.org/10.1016/j.heliyon.2023.e16475

[10] Maruyama, H. (2024). Preparation of adsorbent from mechanochemical reaction-based waste seashell with sodium oxalate and its application in Pb ion adsorption. Surfaces, 7(2), 208-224. https://doi.org/10.3390/surfaces7020014

[11] Muteeb, G., Ansari, K., Eyvaz, M., Farhan, M., Aatif, M., Agrawal, D., El Oirdi, M., & Dehghani, M. H. (2025). Removal of methylene blue (MB) dye from water and wastewater using acid-activated chicken bone in a batch adsorption process. *Scientific Reports*, *15*(1), 23098. https://doi.org/10.1038/s41598-025-08341-3

[12] Nhung, N. T. H., Long, V. Q., & Fujita, T. (2023). A critical review of snail shell material modification for applications in wastewater treatment. Materials, 16(3), 1095. https://doi.org/10.3390/ma16031095

[13] Nkwoada, A. U., Onyedika, G., Oguzie, E.E., Ogwuedgu, M. (2021). Periwinkle Shell Composite Materials in Adsorption and Photocatalysis: A review. Journal of Materials Science Research and Reviews, 8(4):89-1028(4), 89-102.

[14] Nwaeju, C.C., Edoziuno, F.O., Okuma, S.O., Tuaweri, T.J. (2025). Transforming marine waste into valuable resources: Morphological and structural characterization of crab shell particles for composites. BMC Environmental Science, 2(1). DOI:10.1186/s44329-025-00023-9

[15] Pathania, D., Sharma, S., & Singh, P. (2013). Removal of methylene blue by adsorption onto activated carbon developed from Ficus carica bast. *Arabian Journal of Chemistry*, *10*(2), 1445-1451. https://doi.org/10.1016/j.arabjc.2013.04.021

[16] Senthil Rathi, B., Ewe, L. S., Sanjay, S., Sujatha, S., Yew, W. K., Baskaran, R., & Tiong, S. K. (2024). Recent trends and advancement in metal oxide nanoparticles for the degradation of dyes: Synthesis, mechanism, types and its application. Nanotoxicology, 18(3), 272-298. https://doi.org/10.1080/17435390.2024.2349304

[17] Tabassum, S., Sahadat Hossain, M., Bin Mobarak, M., Nigar, F., & Ahmed, S. (2024). Synthesis of nano calcium silicates from waste calcite and aragonite phases for efficient adsorptive removal of industrial organic pollutants. Arabian Journal of Chemistry, 17(7), 105901. https://doi.org/10.1016/j.arabjc.2024.105901